IOPscience iopscience.iop.org

Home Search Collections Journals About Contact us My IOPscience

Impurity transport studies in the Madison Symmetric Torus reversed-field pinch during standard and pulsed poloidal current drive regimes

This content has been downloaded from IOPscience. Please scroll down to see the full text.

2014 Plasma Phys. Control. Fusion 56 075012

(http://iopscience.iop.org/0741-3335/56/7/075012)

View the table of contents for this issue, or go to the journal homepage for more

Download details:
This content was downloaded by: mdnornberg
IP Address: 128.104.165.161
This content was downloaded on 16/05/2014 at 16:16

Please note that terms and conditions apply.

IOP Publishing Plasma Physics and Controlled Fusion

Plasma Phys. Control. Fusion **56** (2014) 075012 (7pp) doi:10.1088/0741-3335/56/7/075012

Impurity transport studies in the Madison Symmetric Torus reversed-field pinch during standard and pulsed poloidal current drive regimes

T Barbui[1], L Carraro[1], D J Den Hartog[2], S T A Kumar[3] and M Nornberg[2]

[1] Consorzio RFX, Padova, Italy
[2] Department of Physics, University of Wisconsin-Madison, Madison, WI, USA
[3] Department of Electrical and Computer Engineering, University of Wisconsin-Madison, Madison, WI, USA

E-mail: tullio.barbui@igi.cnr.it

Received 7 October 2013, revised 31 March 2014
Accepted for publication 22 April 2014
Published 15 May 2014

Abstract

The transport of intrinsic impurities is investigated during standard and improved confinement regimes of the Madison Symmetric Torus (MST) reversed-field pinch. The impurity diffusion coefficient (D) and pinch velocity (v) are obtained through comparing the time evolution of experimental impurity density profiles with the results of a one-dimensional impurity transport code. Experimental hollow fully stripped (C, O, B) ion populations in improved confinement discharges are reproduced with the transport code indicating outward convection of impurity ions. Estimated D and v are low and close to classical values. Standard MST discharges are characterized by a high level of stochasticity and nearly flat radial profiles of the fully stripped carbon. To reproduce this flat impurity profile a high outward convective velocity and high central D are assumed in the simulation.

Keywords: impurities in plasmas, reversed-field pinch, transport properties

(Some figures may appear in colour only in the online journal)

1. Introduction

Impurity transport and particle confinement are key issues in plasma devices. In tokamaks it has been observed that in high confinement regimes, such as H-mode and ITB, impurity density profiles tend to be more peaked than those of the main ion density [1]. This phenomenon, called 'impurity accumulation', is attributed to neoclassical inward convection [2]. It increases radiation losses and radiative instabilities, dilutes the plasma, reduces plasma reactivity, and poses a serious problem in future fusion devices.

Other magnetic configurations show different impurity behaviour. In the LHD heliotron extremely hollow profile of carbon impurity was observed in plasmas with a steep gradient of the ion temperature, due to a strong outward convection driven by the ion temperature gradient [3]. In the RFX-mod reversed-field pinch (RFP) an outward convective velocity was found, producing an external barrier which prevents impurity penetration and accumulation in the core of the plasma [4].

In the Madison Symmetric Torus (MST) RFP density measurements on intrinsic impurities showed similar features. During the improved confinement regime impurities are expelled from the core and the resulting profiles become hollow [5]. This expulsion mechanism was explained by the classical temperature screening effect and the hollow profiles agreed well with classical expectations [6].

In this paper the intrinsic impurity transport in MST is analysed by means of a one-dimensional (1D) impurity transport code. Transport coefficients are estimated through comparing carbon density measurements from charge-exchange recombination spectroscopy (CHERS) with simulated carbon abundances for both standard and improved confinement discharges. Simulated profiles of dominant impurities in MST are used to estimate Z_{eff}.

 © 2014 IOP Publishing Ltd Printed in the UK

2. The device and the simulation model

The MST is a large ($a = 0.52$ m, $R = 1.5$ m), moderate current ($\leqslant$600 kA), RFP device. Its vacuum vessel is aluminum, with a thickness of 5 cm [7]. Partially covering the inner surface of the vessel are tiles and limiters which interact with the plasma during the discharge and become a source of impurities. The identified dominant impurities in MST plasmas are carbon, oxygen, boron and aluminum. Carbon comes from the graphite tiles and limiters which line the vacuum vessel, boron from the boron nitride probes and RF antennas which are routinely inserted and from wall-conditioning through boronization, oxygen from the adsorption of H_2O vapour when MST is brought up to air, and aluminum from the vacuum vessel. The populations of these impurities vary with the plasma regimes which are characterized by different values of electron temperature, density and magnetic field configuration.

During standard discharges multiple coupled tearing modes result in quasi-periodic sawtooth oscillations. Magnetic field lines follow chaotic trajectories and transport is therefore predominantly stochastic [8]. MST operates also in an improved confinement regime where tearing modes are strongly reduced. Such regime is achieved driving a poloidal current at the edge of the plasma through pulsing the toroidal magnetic field. This technique is called 'pulsed poloidal current drive' (PPCD) and reduces the level of magnetic fluctuations, raises the core electron temperature, and increases the confinement time [9–11].

In the past years impurity density measurements were made in MST by means of CHERS. A beam of neutral hydrogen atoms is injected radially into the plasma where neutrals exchange an electron with the impurity ions. The impurity ions are left in an excited lower charge state which then radiatively decays. The charge-exchange process conserves energy, so the Doppler shift and Doppler broadening of the de-excitation emission are used to calculate flow velocity and temperature of the initial-charge-state impurity ion population. Local impurity densities are also calculated from the emission brightness through modelling of the effective emission rates. A 10% uncertainty in the ion impurity densities is considered, mainly due to uncertainties in the beam attenuation calculations and transmission efficiencies of the viewing lenses [12].

The experiments reported in this paper were conducted in deuterium plasmas during both standard and PPCD discharges. Carbon density measurements in standard discharges display nearly flat radial profiles explained by the high diffusion related to the field stochasticity [5]. Carbon density in the core of PPCD discharges, however, decreases after the transition to improved confinement while, in the outer region, the density slowly increases. The profile in the core region ($0 \leqslant r/a \leqslant 0.6$) approaches a hollow shape towards the end of the PPCD phase. Additional CHERS measurements made at higher plasma current reveal that boron and oxygen have a similar behaviour [6].

The impurity density measurements are here reproduced through a 1D impurity transport code coupled to a collisional–radiative code for boron, carbon and oxygen [13]. The model solves the continuity equations for ion states of the different species:

$$\frac{\partial n_z}{\partial t} = -\frac{1}{r}\frac{\partial}{\partial r}(r\Gamma_z) + I_{z-1}n_e n_{z-1} - ((I_z + R_z)n_e + R_z^{cx}n_n)n_z + (R_{z+1}n_e + R_{z+1}^{cx}n_n)n_{z+1} \quad z = 0, \ldots, Z_N \tag{1}$$

where Γ_z is the radial flux density (positive when directed outwards) of the ions of charge $+z$ for the atomic species with nuclear charge Z_N, n_z is the corresponding ion density. For the ions of charge z, I_z is the ionization rate coefficient [14], R_z the recombination rate coefficient (radiative + three-body + dielectronic [15]) and R_z^{cx} the charge-exchange rate coefficient [16]. n_n is the deuterium neutral density. The impurity flux density Γ_z is expressed as the sum of a diffusive and an outward convective term:

$$\Gamma_z = -D\frac{\partial n_z}{\partial r} + vn_z \tag{2}$$

where D and v are the radially dependent diffusion coefficient and outward convection velocity, respectively, both assumed to be independent of the charge of the ions. The continuity equations (1) are initially solved for the ground states of the ions; then, for each radial position, the collisional–radiative model is applied to calculate the steady-state excited level populations of the He-like and H-like ions and finally the absolute intensities of the spectral lines.

Inputs to the code are T_e $(r = 0, t)$ measured by Thomson scattering diagnostic (central chord [17]) and n_e $(r = 0, t)$ from the central line-averaged density measured by the CO_2 interferometer [18]; electron temperature profile, $T_e(r)$, follows the indications from the multi-chord Thomson scattering measurements; electron density profile, $n_e(r)$, is assumed on the basis of FIR interferometry measurements [19]. In standard conditions T_e (r) and $n_e(r)$ are fixed in shape and only their central values evolve in time according to the measurements. In PPCD conditions both $T_e(r)$ and n_e (r) comes directly from the measurements, with a time resolution of 0.5 ms for $T_e(r)$ and 1 ms for $n_e(r)$.

The neutral density profile is calculated using the Monte Carlo neutral particle tracing code NENÈ [20]. This code models the neutral profile whose absolute value is determined through the measured D_α line emission from the edge of the plasma. $n_n(r)$ is fixed in shape; its normalized value is multiplied at any time by n_e $(0, t)$ giving the time evolution.

Impurity influxes (boundary conditions) are tuned to reproduce the time evolution of strong lines from low ionization stages measured by the impurity monochromator array.

The majority ion temperature is a further input: T_i (r) profile is assumed as a multiple of the T_e (r) profile, following the indications of the Rutherford scattering of helium neutrals injected by a diagnostic helium neutral beam [21]. The majority deuterium temperature is quite similar to the minority C^{6+} temperature measured by CHERS [22].

The transport coefficients $D(r)$ and $v(r)$ are estimated by comparing the impurity populations obtained by the simulation with the measured impurity densities: the coefficients are varied until a match is achieved within the experimental

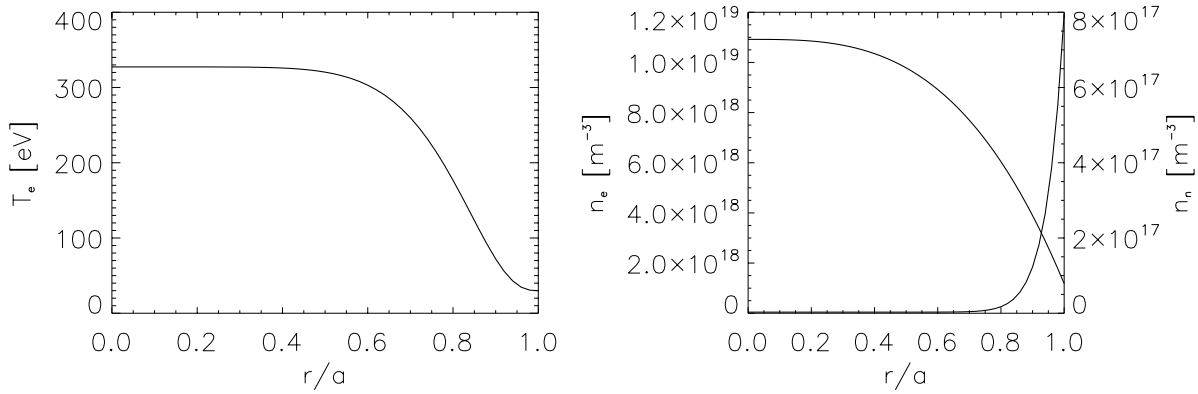

Figure 1. Profiles of electron temperature, electron density and neutral density used to simulate standard plasmas.

uncertainties. Since CHERS impurity profiles consist of few points, D and v profiles are estimated using simple functions, linear between two consecutive spatial nodes (two and three nodes are used for D and v respectively). The simulation is started with $D(r)$ set to constant values for the inner and the outer regions, connected through a step function. $D(r)$ is then adjusted, by modifying the two constant values and shifting the position of the transition. $v(r)$ is simply set in the form $v\,(r) = (r/a)\,v_a$, then the profile is adjusted by adding radial transition points in which $v(r)$ can be set positive (outward convection) or negative (inward convection). The profiles are adjusted until a satisfactory simulation of the fully stripped ion population is achieved. A least-squares procedure is applied minimizing the difference between the simulated and experimental densities. An estimate of the uncertainties in the D and v profiles is obtained from the spread in a set of results of the minimization procedure changing the initial free parameters.

Radial measurements of the impurity densities on MST were averaged over a time interval of some milliseconds and over similar discharges. In standard discharges the C^{6+} density measurements were carried out away from sawtooth events, where a steady-state condition of the plasma can be assumed; they represent equilibrium profiles [5]. In these conditions transport coefficients are estimated by matching the measured density profile with the steady-state profile achieved in the simulation (usually reached after ∼15–20 ms). In a steady-state situation without sources and sinks ($\Gamma_z = 0$ in equations (1) and (2)) only the ratio v/D (peaking factor) can be determined by reproducing the density profile. In our simulation of the standard discharge the condition $\Gamma_z \neq 0$ has been verified, as detailed in the next section, and a separate estimate of the two coefficients has been obtained.

During the PPCD the plasma is not steady-state: T_e is constantly increasing, the impurity influxes and the profiles of T_e and n_e are also evolving throughout the PPCD period. These time evolutions were taken into account in the simulation. In PPCD conditions the time behaviour of the radial impurity content was measured and its reproduction allowed the transport coefficients to be determined separately. In these conditions also the transport coefficients could be a function of time. However the match of the temporal evolution of the impurity content in three radial locations during the PPCD period, along with a full density profile measured at the end of that period, were obtained without varying D and v with time.

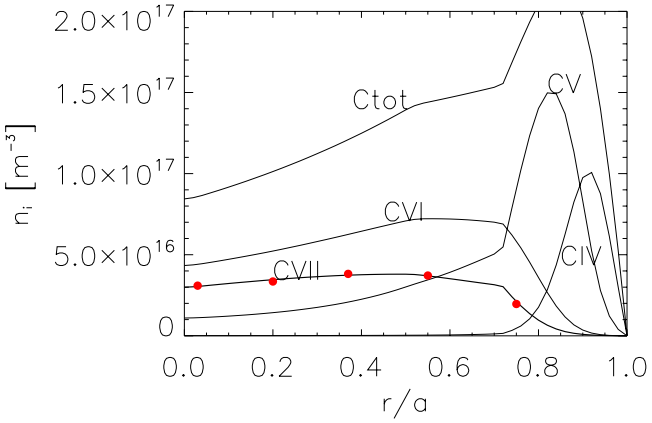

Figure 2. C population profiles computed by the transport code (lines) and C VII density measured by CHERS (red circles) with corresponding error bars. Error bars represent standard deviation of the mean from samples. In this case they are of the order of $\sim 10^{15}\,\mathrm{m}^{-3}$.

3. Impurity transport in standard regime

The procedure described above was applied to 400 kA standard discharges with a typical central electron temperature of 300 eV and electron density of $1 \times 10^{19}\,\mathrm{m}^{-3}$. In figure 1 are shown the profiles of electron temperature, electron density and neutral density used to simulate standard plasmas. Simulated profiles of fully stripped carbon densities were compared with C^{6+} density measurements made away from sawtooth events where the plasma is considered to be in the steady state. This comparison is shown in figure 2 with the best fit D and v. In this type of discharge a neutral profile with low penetration towards the plasma centre was needed in order to reproduce the low C^{6+} content in the outer region. Neutral profile was reconstructed by the NENÈ code. The simulation required a neutral content at $r/a = 0.9$ reduced by a factor of 2.5, still well compatible with the uncertainty of n_n from NENÈ code.

The determined transport coefficients D and v of figure 3 were estimated through the minimization method detailed in section 2. The transport coefficients denote a central region

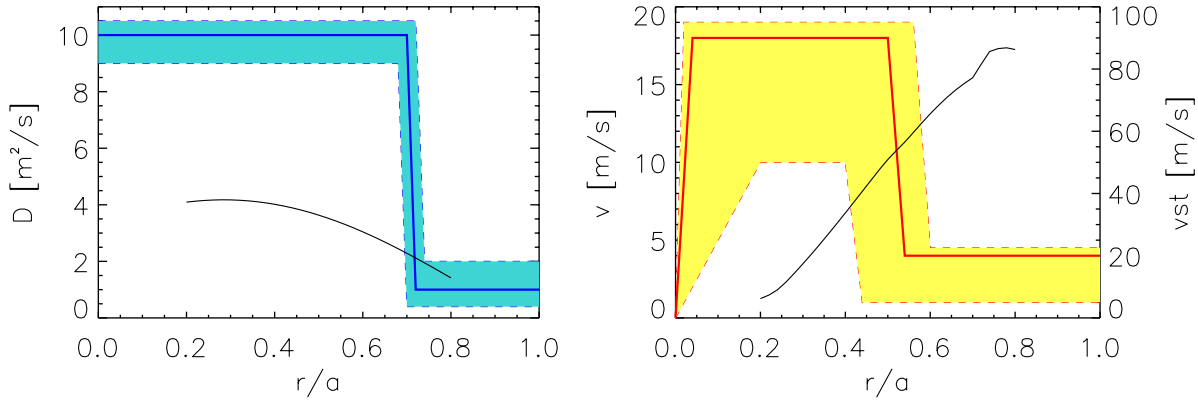

Figure 3. Profiles of the transport coefficients estimated for standard discharge with uncertainty ranges indicated by the respective coloured areas. In black the stochastic coefficients.

with strong diffusion and high outward convection which lead to a nearly flat impurity profile.

A separate estimate of D and v is possible in the considered case, even in the absence of a transient for impurities, due to the presence of source and sink terms in the continuity equations (1) representing atomic physics processes and plasma–wall interactions. The impurity flux is indeed not negligible and the determined peaking factor was found to be not compatible with that obtained from the logarithmic gradient of C^{6+} density profile assuming $\Gamma_z = 0$ in equation (2). The simulation was found to be sensitive to the multiplication of the coefficients by a common factor: dividing or multiplying both D and v beyond the uncertainty regions of figure 3, the match between the simulated and measured fully stripped carbon profile is lost. Moreover, since D and v were used in the first standard-regime part of the PPCD discharge simulation, as described in the next section, if they are divided or multiplied by a common factor beyond the uncertainty regions, the agreement between measurements and simulation in the carbon time evolution during the PPCD period is lost.

Standard discharge in MST is characterized by multiple, coupled tearing modes and the magnetic field lines have a high degree of stochasticity. The calculation of D and v in a stochastic field has been applied and compared with the experimentally determined coefficients. The impurity radial flux through a stochastic magnetic field is proportional to the magnetic diffusion coefficient, which depends on the magnetic fluctuations [23]. The magnetic diffusion coefficient, calculated using the field line tracing code MAL [24], is plotted in figure 4. MAL traces the magnetic field lines given the equilibrium field reconstruction by the code MSTFIT [25] and the mode amplitudes from the resistive MHD code DEBS [26] properly scaled to the mode amplitudes measured at the edge.

The stochastic D and v are plotted in figure 3. Stochastic D is lower than the D estimated through the simulation, but both have their maxima in the core region and then decrease at the edge. Stochastic v is outward all over the radius like the experimental v, but it has its maximum near the edge, contrary to the velocity found with the transport code. Theoretical v is also a factor of 4 greater. It should be noted that the validity of the theoretical calculation of the stochastic coefficients is not valid at $r/a < 0.2$ and $r/a > 0.8$. In those region the system

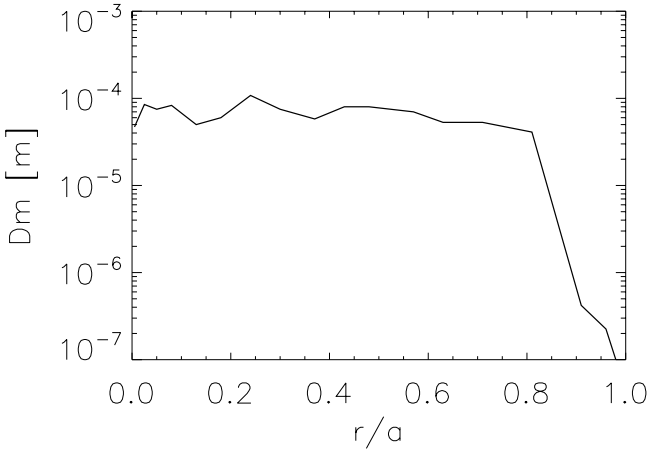

Figure 4. Magnetic diffusion coefficient calculated with the field line tracing code. The values at $r/a < 0.2$ and $r/a > 0.8$ are not valid there since the system is not diffusive in those regions.

described by MAL cannot be considered purely diffusive due to imposed constraints (at the boundary $r = 0$ and near the reversal surface) and the calculation of the magnetic diffusion coefficient is not valid [24].

Summarizing, in standard discharges in the limit of a steady-state analysis, the diffusion coefficient can be considered qualitatively consistent with a diffusive transport driven by the magnetic fluctuations, which are greater in the core region. On the other hand, estimated convective velocity behaves differently from the stochastic calculation.

4. Impurity transport in PPCD regime

In the typical PPCD discharge, after a first part (about 10 ms) where the plasma is in the standard regime, PPCD is activated and the discharge enters the improved confinement regime. In the latter phase tearing modes are suppressed. The electron temperature profile steepens in the outer region of the plasma, and the central electron temperature increases substantially, exceeding 1.5 keV at high toroidal plasma current (>500 kA). Ion temperature does not change significantly. The density profile broadens and becomes hollow. Enhanced confinement minimizes the plasma–wall interaction; hence the neutral influx is greatly reduced and neutral deuterium population

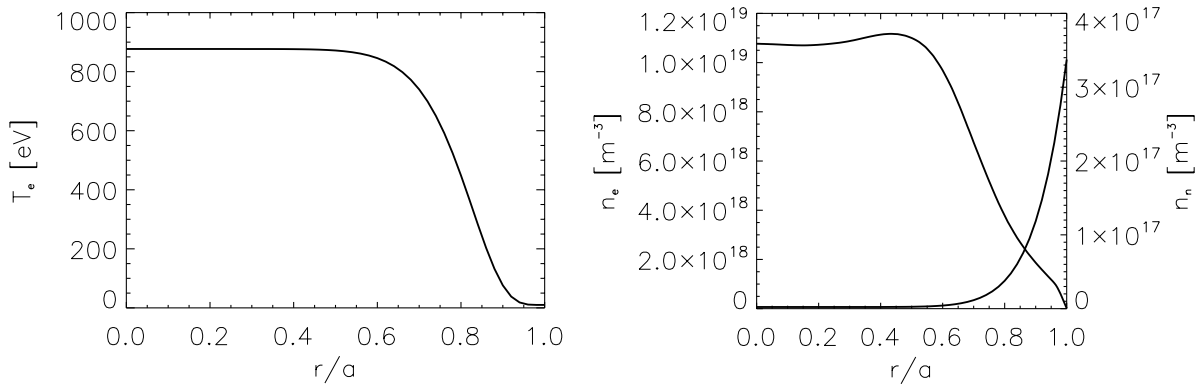

Figure 5. Profiles of electron temperature, electron density and neutral density used to simulate PPCD plasmas.

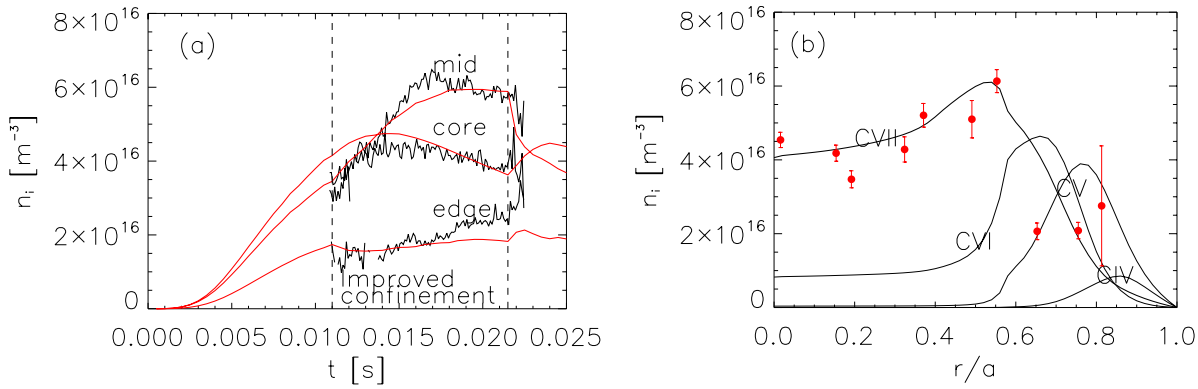

Figure 6. (*a*) C VII population time evolution at $r/a \sim 0.15$ (core), 0.55 (mid), 0.76 (edge), measured (black) and simulated (red). (*b*) C IV–VII population profiles at the end of PPCD computed by the transport code (lines) and C VII density measured by CHERS (red circles) with corresponding error bars. Error bars represent standard deviation of the mean from samples.

drops. This improved regime lasts for about 10 ms and afterwards the discharge returns to the standard regime.

Due to the double regimes in the discharge (standard and PPCD), characterized by different types of transport, two different sets of transport coefficients had to be used for the two phases. At the PPCD activation the simulation changes instantly the D and v profiles in input. For the standard part, the simulation used coefficients similar to those estimated for the standard discharge. For the PPCD period, different coefficients were found by minimizing the difference with the experimental ion densities.

Carbon transport simulations were performed for medium current (400 kA) PPCD discharges with central electron temperature reaching 1 keV during PPCD and electron density about $1 \times 10^{19}\,\mathrm{m}^{-3}$. In figure 5 are shown the profiles of electron temperature, electron density and neutral density used to simulate PPCD plasmas. C^{6+} radial profile towards the end of PPCD is simulated, as well as the impurity density time evolution in three different radial locations, reproducing the measurements carried out through CHERS. The results are shown in figure 6.

The change in the impurity behaviour with the transition to the improved confinement regime is evident. Carbon core content stops growing and starts decaying whereas in the outer part the density is slowly increasing. The stationary flat profile is replaced by one which is hollow in the core region and then suddenly decays approaching the edge.

The estimated transport coefficients required to obtain a good agreement between the simulated density profiles and the experimental data are shown in figure 7. Convective velocity is outward in the core region and then reverses its direction at $r/a \sim 0.7$. Diffusion coefficient is lower in the core and higher in the edge region.

Classical D and v have also been calculated and compared with the experimental transport coefficients. In RFPs the comparable strength of the poloidal and toroidal magnetic fields reduces the connection length in comparison with tokamaks. This results in a sharp decrease of orbit drift, especially regarding the banana width of trapped particles [27]. Classical transport is unaffected by this condition. Neoclassical diffusion therefore tends to be orders lower than the classical one and it can be neglected. Indeed resistive MHD computations showed that transverse diffusion in a RFP is of the same order of classical diffusion of binary collision [28]. However in presence of MHD fluctuations with high stochasticity theoretical calculations showed that particle diffusion is much higher than classical or neoclassical expectations due to anomalous transport [29].

The radial flux of impurity ions due to Coulomb collisions with main ions and other impurity ions was computed for the case of PPCD discharges with suppressed magnetic fluctuations [30]. The uncertainty of this calculation was estimated to be around 10%, due to experimental uncertainties of ion density measurements and to the uncertainty of

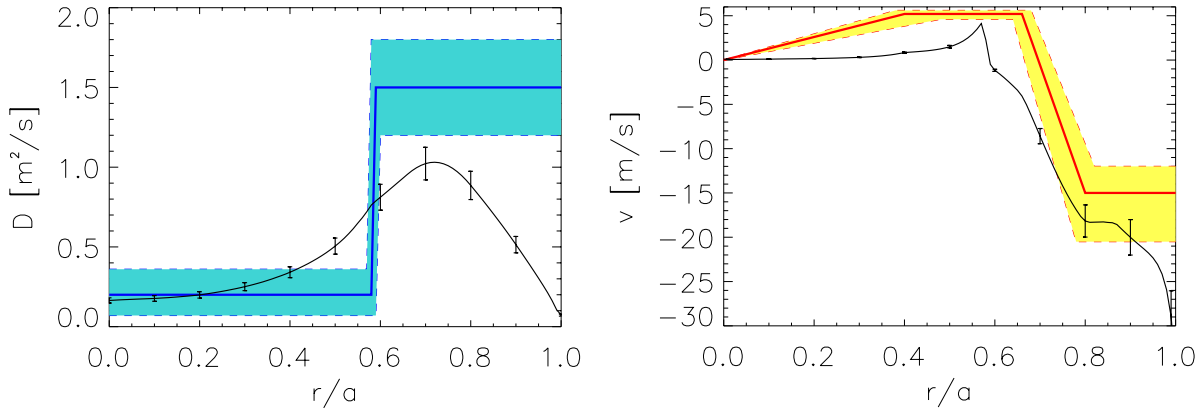

Figure 7. D and v profiles estimated for the PPCD regime with uncertainty ranges indicated by the respective coloured areas. In black the classical coefficients for carbon with ±10% error bars.

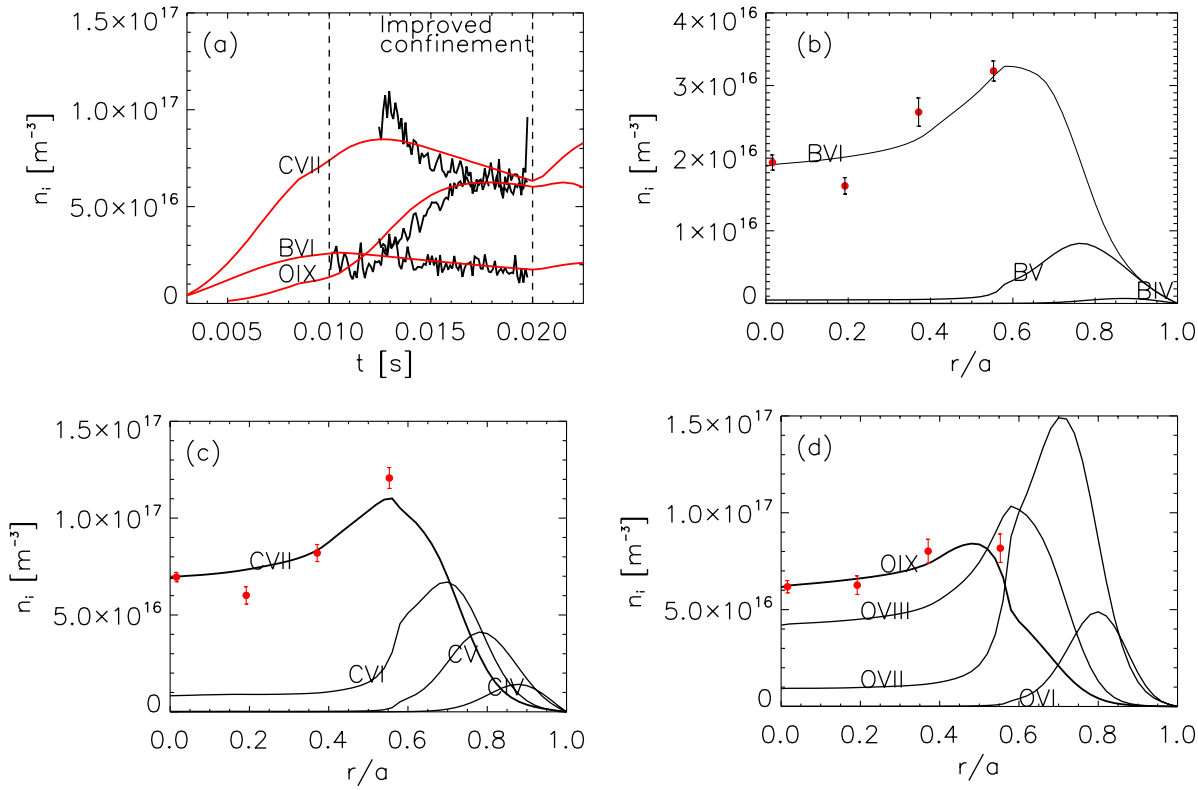

Figure 8. (*a*) B VI, C VII, O IX density time evolution at the core measured (black) and simulated (red). B IV–VI (*b*), C IV–VII (*c*) and O VI–IX (*d*) population profiles towards the end of PPCD computed by the transport code (lines) and B VI, C VII, O IX density measured by CHERS (red circles) with corresponding error bars. Error bars represent standard deviation of the mean from samples.

the Coulomb logarithm value in the collision frequency expression. The experimental transport coefficients agree within a factor lower than 2 with the classical calculation in the region of the profile which is constrained by CHERS data. So it is possible to conclude that impurity transport in MST during PPCD is nearly classical.

The mechanism involved in the impurity expulsion after the transition to the improved confinement is the classical temperature screening effect in which the ion temperature gradient drives an outward flux of impurities [6, 30].

Complementary simulations of higher current (550 kA) PPCD discharges were performed. Typical parameters are central electron temperature exceeding 1.5 keV during PPCD and electron density of about $8 \times 10^{18}\,\mathrm{m}^{-3}$.

In high current discharges experimental measurements of fully stripped ion densities of boron and oxygen are available in addition to carbon. Thus B, C, O codes were run to simulate all three species behaviours. Figure 8 shows the results of these simulations. Radial profiles of the populations of boron, carbon and oxygen were reproduced along with the time evolutions of the fully stripped ion core content. As for medium current PPCD discharges, fully stripped ions assume a hollow profile towards the end of the improved confinement regime. Core density decreases soon after the transition for both boron and carbon, whereas oxygen continues to grow and starts decreasing only at the very end of the improved confinement period, assuming a final profile less hollow than other species.

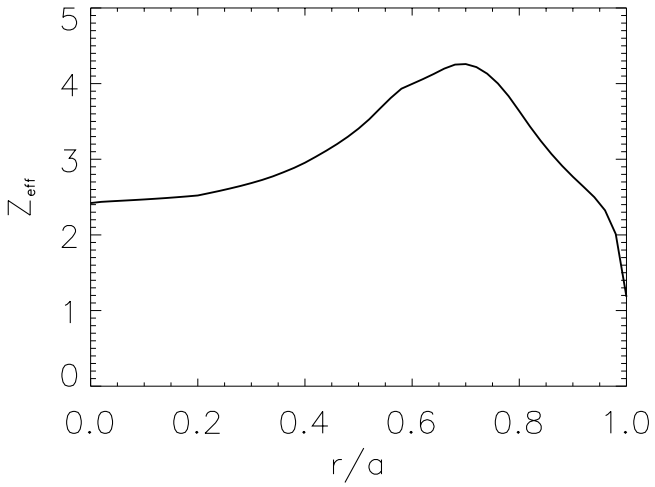

Figure 9. $Z_{\rm eff}$ computed by the code with contributions of B, C, O and Al.

These simulations were obtained by using the same transport coefficients of figure 7 estimated for carbon during the improved confinement phase. The coefficients reproduce the impurity densities for species with different Z implying that the impurity transport is not strongly dependent on mass/charge, at least for ions with similar Z.

In figure 9 the profile of $Z_{\rm eff}$ was obtained adding to the populations of B, C and O simulated by the codes the contribution of Al ions from CHERS measurements. Al density measurements found a concentration of the dominant Al^{11+} ion of the order of $2 \times 10^{16}\,{\rm m}^{-3}$ [12]. $Z_{\rm eff}$ profile agrees with previous estimate from x-ray measurements and modelling which ranged from 4 to 6 [31]. Moreover, it is being used as a benchmark for SXR tomography modelling [32].

5. Conclusions

Impurity transport in MST has been analysed in both standard and improved confinement regime. The results were obtained through simulations with a 1D impurity transport code of experimental impurity density measurements.

The analysis reveals a different nature of impurity transport between standard and PPCD discharge in MST. The estimated transport coefficients in the two cases differ by one order of magnitude and have very different features.

In standard plasmas transport is anomalous, with very high diffusion in the central region, resulting in nearly flat radial profiles of the fully stripped ion. A high flat D was assumed in the simulation, qualitatively consistent with the theoretical indications from the stochastic diffusion.

During PPCD magnetic fluctuations are reduced; impurity density evolves into a hollow radial profile, indicating outward convection of impurity ions. Estimated transport coefficients are low and close to classical values. Convective velocity is outward in the core region and then reverses its direction at mid-radius. Additionally, high current PPCD simulations involving other species evidence the same transport and a mass/charge independence of the transport parameters.

References

[1] Dux R, Giroud C, Neu R, Peeters A G, Stober J and Zastrow K-D 2003 *J. Nucl. Mater.* **313–316** 1150
[2] Hirshman S P and Sigmar D J 1981 *Nucl. Fusion* **21** 1079
[3] Yoshinuma M *et al* 2009 *Nucl. Fusion* **49** 062002
[4] Menmuir S, Carraro L, Alfier A, Bonomo F, Fassina A, Spizzo G and Vianello N 2010 *Plasma Phys. Control. Fusion* **52** 095001
[5] Kumar S T A, Den Hartog D J, Magee R M, Fiksel G and Craig D 2011 *Plasma Phys. Control. Fusion* **53** 032001
[6] Kumar S T A *et al* 2012 *Phys. Plasmas* **19** 056121
[7] Dexter R N, Kerst D W, Lovell T W, Prager S C and Sprott J C 1991 *Fusion Technol.* **19** 131
[8] Chapman B E, Almagri A F, Cekic M, Den Hartog D J, Prager S C and Sarff J S 1996 *Phys. Plasmas* **3** 709
[9] Chapman B E *et al* 2002 *Phys. Plasmas* **9** 2061
[10] Sarff J S, Hokin S A, Ji H, Prager S C and Sovinec C R 1994 *Phys. Rev. Lett.* **72** 3670
[11] O'Connell R *et al* 2003 *Phys. Rev. Lett.* **91** 045002
[12] Kumar S T A, Den Hartog D J, Chapman B E, O'Mullane M, Nornberg M, Craig D, Eilerman S, Fiksel G, Parke E and Reusch J 2012 *Plasma Phys. Control. Fusion* **54** 012002
[13] Mattioli M, Fournier K B, Puiatti M E, Valisa M, Carraro L, Coffey I, O'Mullane M, Sattin F and Scarin P 2002 *Plasma Phys. Control. Fusion* **44** 33
[14] Bell K L, Gilbody H B, Hughes J G, Kingston A E and Smith F J 1983 *J. Phys. Chem. Ref. Data* **12** 891
[15] Pal'chikov V G and Shevelko V P 1995 *Reference Data on Multicharged Ions* (Berlin: Springer)
[16] Phaneuf R A, Janev R K and Pindzola N F 1987 Collisions of carbon and oxygen ions with electrons, H, H_2 and He *Atomic Data for Fusion* vol 5 *Oak Ridge National Laboratory Report* ORNL-6090
[17] Reusch J A, Borchardt M T, Den Hartog D J, Falkowski A F, Holly D J, O'Connell R and Stephens H D 2008 *Rev. Sci. Instrum.* **79** 10E733
[18] Innocente P, Martini S and Ferrer Roca Ch 1992 *Rev. Sci. Instrum.* **63** 4999
[19] Brower D L, Jiang Y, Ding W X, Terry S D, Lanier N E, Anderson J K, Forest C B and Holly D 2001 *Rev. Sci. Instrum.* **72** 1077
[20] Lorenzini R, Auriemma F, Canton A and Carraro L 2006 *Phys. Plasmas* **13** 112510
[21] Den Hartog D J *et al* 2006 *Rev. Sci. Instrum.* **77** 10F122
[22] Sarff J S *et al* 2003 *Plasma Phys. Control. Fusion* **45** A457
[23] Hsu J Y, Harvey R W and Wong S K 1981 *Phys. Fluids* **24** 2216
[24] Hudson B 2006 Fast ion confinement in the reversed-field pinch *PhD Thesis* University of Wisconsin-Madison
[25] Anderson J K, Forest C B, Biewer T M, Sarff J S and Wright J C 2004 *Nucl. Fusion* **44** 162
[26] Schnack D D, Barnes D C, Mikic Z, Harned D S and Caramana E J 1987 *J. Comput. Phys.* **70** 330
[27] Wakatani M and Itatani R 1973 *J. Phys. Soc. Japan* **34** 181
[28] Oshiyama H and Masamune S 1983 *J. Phys. Soc. Japan* **52** 2041
[29] Chen T S, Nagata A, Sato K, Ashida H and Amano T 1992 *J. Phys. Soc. Japan* **61** 530
[30] Zhdanov V M 2002 *Transport Processes in Multicomponent Plasma* (London: Taylor and Francis)
[31] Clayton D J, Almagri A F, Burke D R, Forest C B, Goetz J A, Kaufman M C and O'Connell R 2010 *Rev. Sci. Instrum.* **81** 10E308
[32] McGarry M B 2013 Probing the relationship between magnetic and temperature structures with soft x-rays on the Madison Symmetric Torus *PhD Thesis* University of Wisconsin-Madison